XVI SIMPOSIO INTERNACIONAL SELPER 2014

La geoinformación al servicio de la sociedad

MEMORIAS

SOCIEDAD LATINOAMERICANA DE PERCEPCIÓN REMOTA Y SISTEMAS DE INFORMACIÓN ESPACIAL

SELPER COLOMBIA 30 AÑOS

Medellín , Colombia

29 de Septiembre al 3 de Octubre de 2014

A simple method for mapping annual agricultural areas by analyzing MODIS Land Surface Temperature time-series

Denis Araujo Mariano*[1], William Foschiera[2], Maurício Alves Moreira[3]

Remote Sensing Division (DSR), National Institute for Space Research (INPE), Av. dos Astronautas, 1758, São José dos Campos, CEP: 12227-010, SP, Brazil

*1 – Corresponding author email: denis.mariano@usp.br
2 – Email: wfoschiera@gmail.com
3 – Email: mauricio@dsr.inpe.br

The current paper presents a method for mapping summer annual agriculture (maize and soybean) by analyzing Land Surface Temperature (LST) time-series derived from the Moderate Resolution Imaging Spectroradiometer (MODIS). We used Terra and Aqua LST daytime and nighttime data (M_D11A2) with 8-day temporal and 1km spatial resolution. The physical basis behind the method is the heat transfer between soil, plant and atmosphere over time. There are two approaches, inter-daily and intra-daily LST variation. We tested daytime and day-night difference time-series, being the latter more efficient on detecting annual agriculture. Regarding the satellites, Aqua proves on being more efficient due the passage hour for daytime. In sense, the couple Difference/Aqua yielded better results. However, the performance is strongly dependent on the contiguity of agricultural areas due to the high thermal mixing susceptibility. Another drawback is the spatial resolution (1 km) which depending on the situation fails on detecting low acreage crops. Despite the limitations, the idea shows potential to be coupled to traditional vegetation indices based methods for furthering the biophysical meaning and relationships between vegetation and remote sensing. It also brings new findings about vegetation thermal behavior throughout the time.
Keywords: land surface temperature; agriculture; MODIS; time-series.

1. Introduction

Agriculture is one of the main sources of income in most of the developing countries and due to the increasing need for raw materials and food; this activity is always evolving in technology and more intensively in acreage. In Brazil, the agriculture chain represents about a quarter of the Gross Domestic Production (CEPEA, 2014) and albeit facing a decreasing in the rate of acreage expansion, it does still existing. For detecting and measuring these dynamics, Remote Sensing techniques have been proven on being fast and

accurate way to deliver statistics about the acreage and crop conditions on time.

In this sense, several works deal with mapping annual crop areas using direct image interpretation, which is based on the interpreter knowledge about the crops and datasets (Rudorff *et al*., 2011). Another common technique is based upon vegetation indices (VI) and many works use one or combinations of many (Wardlow & Egbert, 2008). The VIs most commonly used for these purposes are the Normalized Difference Vegetation Index (NDVI) (Rouse, Haas, & Schell, 1974) and Enhanced Vegetation Index (EVI) (Huete *et al*., 2002). These VIs and many other are based on the relationship between the red and near infra-red channels showing the contrast between the high radiation absorption by the chlorophyll in the red channel and high reflectivity by the leaf structure and its components on near infra-red channel (Tucker, 1979).

Both techniques are not straightforward by using medium or coarse resolution images due to the fast dynamic of the crop growing and the difficulty of crop detection in a single image. For overcoming these issues interpreters rely upon multitemporal images analysis. In this way it is possible to compare the growing of vegetation since the bare soil or straw aspect to the maximum leaf area index (LAI) and even to the senescence stage.

In the south of Brazil, the sowing of summer rainfed agriculture of soybean and maize usually takes place from October to December and the harvest occurs during the first three months of the next year. Farmers use to do double cropping even for rainfed agriculture by rotating usually from soybean to maize or wheat. Irrigated agriculture has a more flexible sowing season due to the lower dependency on the precipitation rates. This latter case can sometimes leads the interpreters to neglect an area of high biomass (high LAI, high VI) due to the epoch of occurrence as they were expecting to detect bare soil or straw cover.

Albeit the above mentioned techniques are well consolidated and have proven their effectiveness, in some situations they can fail or be highly time-consuming depending on the method and experience of the interpreter. In sense, these techniques rely only upon optical remote sensing channels. However, the thermal analysis approach for mapping purposes was not deeply investigated yet. A comprehensive work of land cover classes discrimination and change analysis was performed by Lambin & Ehrlich (1996), they coupled NDVI and LST data from the Advanced Very High Resolution Radiometer (AVHRR) and analyzed 10 years of data for the African continent showing that the use of LST improves the capacity to discriminate land cover classes as compared to NDVI applied solely. Nemani & Running (1997) compared the correlation between NDVI and LST derived data from AVHRR for different LCCs yielding good agreement. Nonetheless, the mentioned studies were developed always coupling traditional VIs to LST data. Indeed, the biophysical meaning of LST was not in depth explored being often overshadowed by VIs high efficiency.

The physical basis behind it explores the difference between the emissivity of the soil and the plant canopy. According to Tang & Li (2014), land surface emissivity is the effectiveness of a surface on emitting thermal radiation, and spectral emissivity is the ratio of energy radiated by a particular material to energy radiated by a black body at the same temperature. Another property of the material is the thermal inertia (TI) which is the resistance to temperature variations; it is defined in function of the material's specific heat capacity, thermal conductivity and bulk density. Water has a high TI which makes its temperature fluctuation slow when compared to other common surface materials. For this reason, water bodies can be heater than the neighbour land surface during the night. Crop

canopies have higher TI than dry soil showing lower diurnal temperature variation due to the content of water in its leaf structure. Moreover, as observed by Murray & Verhoef (2007), the vegetation canopy significantly influences the soil heat flux by reducing the irradiance reaching the soil surface during the day and acting as an insulator barrier between soil and atmosphere during the nighttime.

The Land Surface Temperature products provided by sensors onboard satellites are mainly dependent on the object's albedo, emissivity, thermal inertia and exogenous factors such as wind and relief (Kuenzer & Dech, 2013). However, LST is highly inverted correlated to the target moisture coupled with its intrinsic properties, therefore, LST products have been used in applications for drought detection concerning or not to agriculture. Wan *et al*. (2004) used LST and NDVI combined for monitoring drought in the USA. Many other works have applied LST solely or combined with other VIs and even precipitation data for detecting and monitoring drought on a multitemporal approach (Ezzine, Bouziane, & Ouazar, 2014; Kogan, 1995; Rhee, Im, & Carbone, 2010).

The present work is based on the assumption that LST is suitable for mapping annual agriculture due to the different thermal properties of the targets throughout the season by relying on time-series analysis in a simplified manner. The main objective is to establish a conceptually and computationally straightforward method for discriminating annual agriculture from other LCCs by analyzing LST time-series data from the sensors MODIS onboard Terra and Aqua satellites. The specific objectives are: *i)* characterize the LST temporal behavior of the LCCs; *ii)* assessment of spatial agreement between LST derived classification and reference map.

2. Materials and methods

2.1. *Study area*

The study focused on the Northwest, Central-North, Central-West and West mesoregions of Paraná state, which is located in the south of Brazil, however, the analysis were performed by municipality and then aggregated into microregions. The three latter regions comprise the traditional and most important grain production area of the state which occurs mostly on clay texture soils. During the last two decades the Northwest region has shown an expansion of sugarcane on areas of medium texture soils. Nonetheless, a few sugarcane expansion areas can be found on the Central-North area. Albeit being traditional grain areas, the region was chosen due to two factors: agricultural acreage expansion during the last fifteen years and diversity of farm sizes tending to difficult the mapping, so that being a good area to test the methodology proposed in this work.

2.2. *Base datasets*

The summer crops base map for the 2011/2012 was elaborated by the Insurance and Risk Studies Group (GESER/ESALQ-USP - *www.esalq.usp.br/geser*) using Landsat-TM and ETM+ images visual interpretation and classification of soybean and maize areas. In the present work, we are considering as summer crops maize and soybean whose areas were summed for composing the summer crop area for each year. Other crops coexist in the region; however, the acreage of them is too small as compared to maize and soybean. So, GESER/ESALQ-USP map is highly suitable for the current study, as it considers only soybean and maize areas.

A soil map at the scale of 1:50000 was elaborated by the Brazilian Agricultural

Research Corporation (EMBRAPA) and is available at *www.itcg.pr.gov.br*. In the studied region there is a predominance of Latosols followed by Argisols. Soybean and maize are produced almost totally on clay soils (Argisols, Latosols, Neosols and Nitosols) and sugarcane on medium texture soils (Latosols and Argisols). The Figure 1 depicts the microregions and soil classes for the studied area.

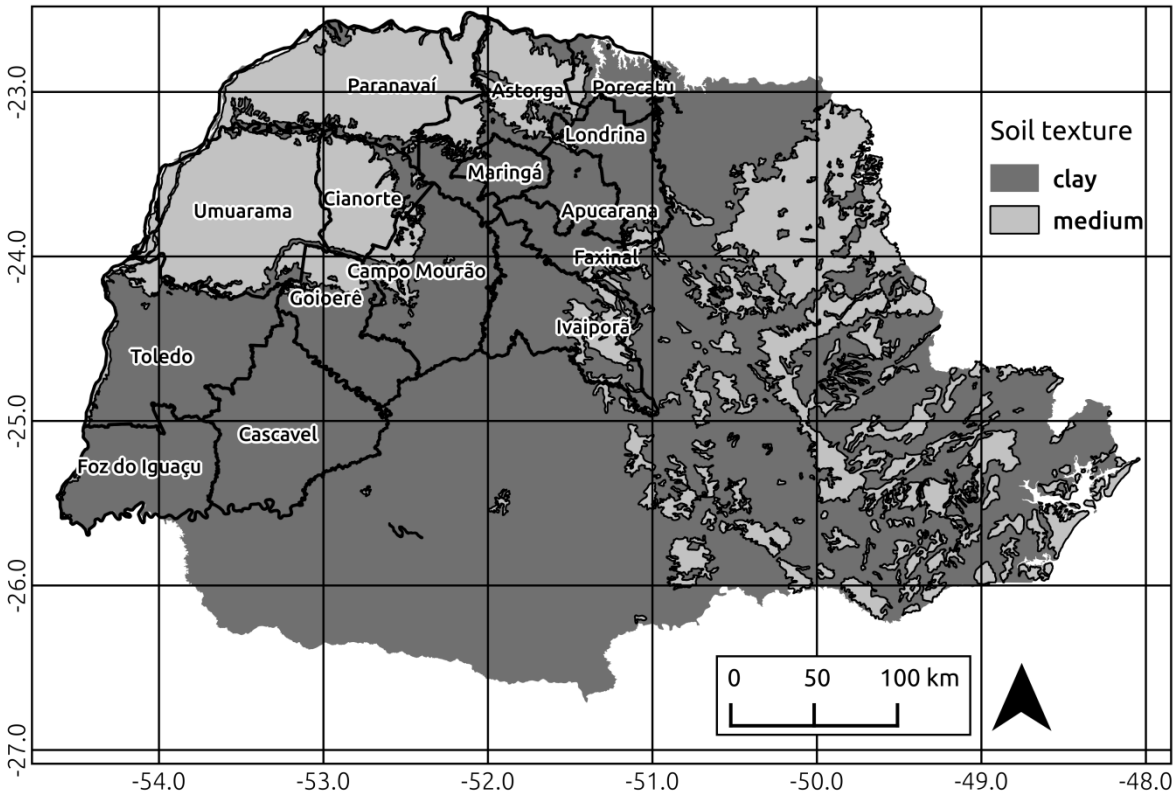

Figure 1 - Study area.

2.3. ***MODIS LST datasets***

Wan & Li (1997) proposed an algorithm to retrieve land surface temperature for day and night passages of the so forthcoming sensor MODIS. Since then, the LST product has been refined being at the present moment in the version 5. According to Wan (2008), the LST products were heavily assessed through calibration and testing campaigns resulting in

errors of about 1°C. For the current work, series of LST data from September to March from 2002 to 2012 were analyzed for both Terra (morning) and Aqua (afternoon) were used. The MOD11A2 (Terra) and MYD11A2 (Aqua) are 8-day compositions of LST from the daytime and nighttime, and emissivity of bands 31 (10780 – 11280nm) and 32 (11770 – 12270nm), all of them at 1km nominal spatial resolution. In this study we used LST day and nighttime data from both satellites.

All the images were firstly reprojected to geographic/WGS84 using the MODIS Reprojection Tool. Then, the files were organized for posterior processing by a Python script that was designed to compute the difference of LST between Day and Night for each 8-day image (hereafter LST-Difference). The Python script is available in our repository at *www.bitbucket.org/geopaitos/python-remotesensing*. The rationale behind that is that greater temperature differences indicate dryer surfaces or lower LAI or both (Sandholt, Rasmussen, & Andersen, 2002). As we are concerned on developing a simple methodology for mapping crops using LST, the Day datasets (hereafter LST-Day) were also analyzed solely by focusing only on the variation between days rather than intra-day.

2.4. *Temporal profiles of LST-Day and LST-Difference for LCCs*

In this step, the seasonal profiles of LST-Day and LST-Difference for each LCC were analyzed, there are four cases: LST-Day and LST-Difference for Terra and Aqua. In order to minimize the latitudinal variation of irradiance, the samples were acquired at about the same latitude (-23°40' to -25°10').

The soil classes were summarized into clay and medium texture due to the intrinsic capacity of water retention which is a key factor for heat transferring between surfaces.

Within the study region, not all the LCCs occurs on the two considered soil types, so that, only sugarcane, forest and annual agriculture were analyzed for both soil classes and pasture only for the medium texture soils. Moreover, the annual agriculture on medium texture soils is seldom verified, due to this the samples may carry great uncertainty derived from the intrinsic heterogeneity and small acreage. Additionally, a special care was taken on sampling Forests, based on the assumption of its LAI steadiness over a season, an ancillary image of EVI was used for selecting Forests whose EVI were similar among samples despite of the soil class. For each of the four cases, the Pearson correlations between the seven LCCs' were calculated and the time-series plots visually analyzed.

2.5. Using season statistics images for mapping and validation

The dataset was grouped from the DOY 185-2011 to DOY 105-2012. Considering that the sowing period for the region ranges from September (maize) or October (soybean) to December and the harvest from January to March, a small extra period was included as pre-sowing window for catching safely the bare soil or straw cover phase.

The metrics combination (LST-Day or LST-Difference) with satellite (Terra or Aqua) that yielded better results (session 3.1) were used for mapping and hence validation. The measure adopted for assessing the LST variation for both intra and inter-daily throughout the time-series is the variance. In this sense, a steady land cover class (e.g. Forest) is likely to show lower phenology variance than agriculture during a given season, due to this, variance can be a good measure to assess the phonological steadiness. For the studied season the variance was calculated in a pixel basis resulting in one variance (σ^2) image for the season. The metrics combination (LST-Day or LST-Difference) with satellite (Terra or

Aqua) that yielded better results (session 3.1) was classified to retrieve the Annual-clay acreage. The classification process was a simple density slice applied in the variance image and the thresholds to separate the Annual-clay class were adjusted manually.

The validation scheme was the simply comparison between the yielded and GESER/ESALQ-USP maps. The outputs for the analysis are a difference map and contingency tables. However, accuracy assessment of maps derived from coarse resolution images, as observed by (Xiao *et al*., 2005) is a daunting task due to the LCCs fragmentation and spectral-mixing in the pixel. The base map was elaborated over TM and ETM+ images whose spatial resolution is about 30m whereas the MODIS LST images used has 1000m resolution.

3. Results and discussion

3.1. *LST-Day and LST-Difference temporal profiles for LCCs*

The temporal profiles for all LCCs were plotted using splines for LST-Day and LST-Diff from Terra and Aqua satellites (Figure 2). The use of splines was convenient for better visualizing these plots, either way, the correlation matrices and variances were calculated using the raw data.

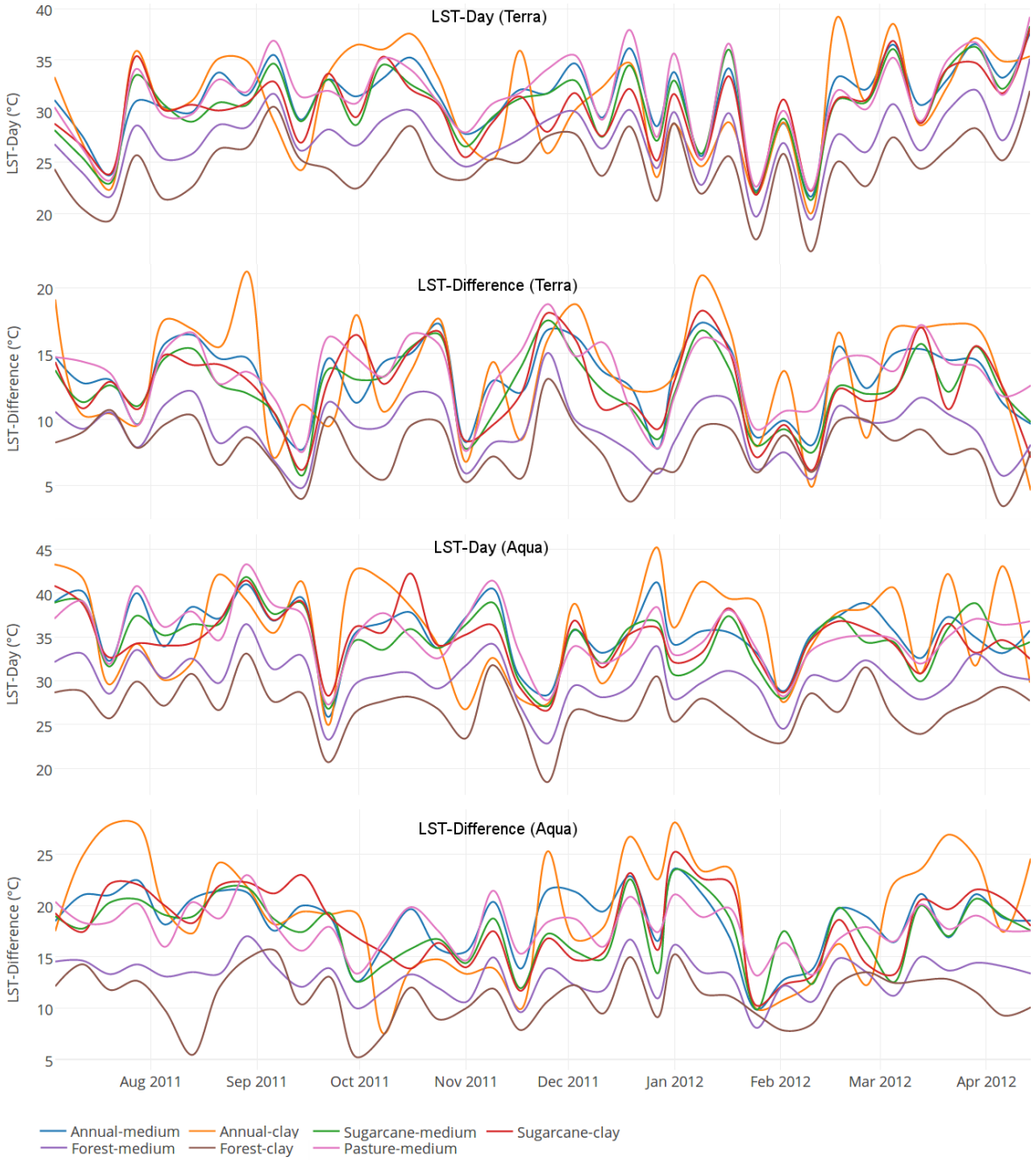

Figure 2 - LST-Day and LST-Difference time series for LCCs

Even though not all LCCs are representative over the considered soil types, Forest-clay and Forest-medium could be used efficiently to assess the soil texture influence on the LST behaviour throughout the season. As observed in the Figure 2, for all combinations the

separation between Forest and the other targets were clear and effective, moreover, the Forest-clay class usually presented lower LST-Day and LST-Difference than Forest-medium. This let us assume that clay textures lead to slower heat transferring between surfaces due to its higher water retention capacity than of the medium texture soils (Murray & Verhoef, 2007). As we are not concerned on assessing the LST data quality which has been already assured (Wan, 2008), it is unnecessary to rely on meteorological stations temperature data, hence, the Forest behaviour throughout the season serves as a comparative pattern for the other classes. Considering that assumption and analyzing the Figure 2, we observed a reasonable correlation among the other LCCs and Forests. The variances of all time-series are presented in the Table 1 and the pairwise Pearson correlation matrices for the four combinations are presented in the Table 2.

Table 1 - LCCs time-series variances.

	Terra – Day	Terra – Difference	Aqua – Day	Aqua – Difference
AM	14.604	8.224	12.646	10.153
AC	26.415	19.715	32.234	33.226
SC	15.953	10.323	12.634	14.404
SM	14.869	7.654	12.316	10.861
FC	10.739	4.622	8.041	6.509
FM	11.188	5.147	8.619	3.771
PM	17.584	7.587	12.259	5.381

A = Annual, S = Sugarcane, F = Forest and P = Pasture. M = medium and C = clay.

As observed in the Table 1, the Annual-clay class shows the higher variance for all the four cases whereas Forest classes show the lowest variances as expected. The odd output is the class Annual-medium whose variance differs considerably from the Annual-clay. However, the Annual-medium class as previously mentioned is unlikely to exist in the study area; therefore, the samples are too small due to the limited acreage. Additionally, as

annual agriculture is not traditional in the medium texture area, the sowing and harvest dates do not follow a strict pattern since they are higher dependent on the rain occurrence during the expected sowing season. For these reasons, the Annual-medium class analysis is inconclusive. Other important observation is in how the variance between classes differs in each of the four cases. The Aqua-Difference combination yielded the highest amplitudes between Annual-clay class and the other classes. This is a key factor for the proposed mapping method effectiveness which relies on variance or standard deviation of a time-series to detach the Annual-clay from a group of classes. Although out of the scope of this work, the observations show that sugarcane variance was greater than for pasture, this is due to a possible occurrence of sugarcane harvest/planting event during the season, which does not occur for pastures.

Table 2 - Pearson correlation between LCCs.

	LST-Day (Terra)							**LST-Difference (Terra)**						
	AM	**AC**	**SM**	**SC**	**FM**	**FC**	**PM**	**AM**	**AC**	**SM**	**SC**	**FM**	**FC**	**PM**
AM	1.000	0.774	0.887	0.946	0.885	0.954	0.945	1.000	0.743	0.897	0.840	0.875	0.637	0.851
AC	0.774	1.000	0.786	0.693	0.573	0.687	0.650	0.743	1.000	0.624	0.734	0.578	0.400	0.518
SM	0.887	0.786	1.000	0.948	0.783	0.894	0.880	0.897	0.624	1.000	0.938	0.877	0.636	0.891
SC	0.946	0.693	0.948	1.000	0.871	0.953	0.963	0.840	0.734	0.938	1.000	0.799	0.568	0.773
FM	0.885	0.573	0.783	0.871	1.000	0.951	0.928	0.875	0.578	0.877	0.799	1.000	0.847	0.903
FC	0.954	0.687	0.894	0.953	0.951	1.000	0.972	0.637	0.400	0.636	0.568	0.847	1.000	0.716
PM	0.945	0.650	0.880	0.963	0.928	0.972	1.000	0.851	0.518	0.891	0.773	0.903	0.716	1.000

	LST-Day (Aqua)							**LST-Difference (Aqua)**						
	AM	**AC**	**SM**	**SC**	**FM**	**FC**	**PM**	**AM**	**AC**	**SM**	**SC**	**FM**	**FC**	**PM**
AM	1.000	0.613	0.883	0.821	0.916	0.813	0.870	1.000	0.637	0.797	0.704	0.815	0.598	0.775
AC	0.613	1.000	0.507	0.693	0.503	0.487	0.457	0.637	1.000	0.612	0.736	0.551	0.490	0.479
SM	0.883	0.507	1.000	0.858	0.906	0.739	0.878	0.797	0.612	1.000	0.871	0.890	0.562	0.765
SC	0.821	0.693	0.858	1.000	0.768	0.660	0.716	0.704	0.736	0.871	1.000	0.736	0.486	0.602
FM	0.916	0.503	0.906	0.768	1.000	0.880	0.943	0.815	0.551	0.890	0.736	1.000	0.692	0.856
FC	0.813	0.487	0.739	0.660	0.880	1.000	0.813	0.598	0.490	0.562	0.486	0.692	1.000	0.588
PM	0.870	0.457	0.878	0.716	0.943	0.813	1.000	0.775	0.479	0.765	0.602	0.856	0.588	1.000

A = Annual, S = Sugarcane, F = Forest and P = Pasture. M = medium texture and C = clay texture.

When analyzing the Table 2, it is clear the lower correlation between Annual-clay and all the other classes, even Annual-medium whose samples fails on representativeness. Amongst the four cases, the pair Aqua-Difference yielded overall lower correlations between classes and as observed in the Table 1, highest variance for Annual-clay.

Some factors explain such behaviour differences between the four combinations. The use of nighttime data presents an information gain about the land surface. As reported by Wang *et al*. (2006), difference between day and night temperatures can be closely related to the surface moisture. In our case, the surface moisture comprises both soil and plant. Since health vegetation together with its LAI is also correlated with moisture, the LST-Difference can also be related to the canopy and soil moisture together. For these reasons, LST-Difference yielded better results than LST-Day.

Regarding the difference in the performance between Terra and Aqua datasets, there are some reasons for that. The Terra satellite acquire images from the land about 10:30 and 22:30 whereas Aqua at 13:30 and 1:30. This means that at the moment of the Aqua passage during the day the land received 3 more hours of irradiance than when Terra passes. Moreover, these 3 hours are indeed the most intensive which means closer to solar nadir. This can be observed when comparing the LST-Day plots of Terra and Aqua (Figure 1) where the latter usually presents higher values.

3.2. *Mapping performance and validation*

To validate the proposed method, we compared the maps provided by GESER/ESALQ-USP to the one produced from the variance image. However, several factors tend to ruin such analysis. As previous mentioned, the difference between spatial resolutions (30m to

1000m) leads to serious incoherencies, as is not expected that a coarse resolution sensor detects as agriculture pixels which annual agriculture percentage acreage is small as compared to the pixel size. Another hurdle for the method performance is the inability on detecting small Riparian forests whose width usually ranges from 30 to 500 m in the study region. These forests exert strong influence on the thermal response of the surrounding areas tending to decrease the method effectiveness.

The percentage of agreement between base and produced map is not straightforward comparable. There are some municipalities where soybean/maize is almost inexistent, then, a simple commission error leads to great percentage error. Due to this reason, we adopted a particular approach to analyze the results, rather than only tables, we preferred to present choropleth and difference maps. The percentage analysis can be a misleading approach, nevertheless, it allows us to draw conclusions regarding to the regions where there are anomalous occurrences. The Figure 3 depicts the percentage error of the agreement between the base and yielded maps by municipality.

The Figure 3 analysis shows clearly that both the commission (lower than 100%) and omission errors (higher than 100%) occur in areas of low agriculture acreage and municipality area ratio. With regards to agreement, the map derived from LST fails where no or few annual agriculture areas exist. This is caused due to the inaptitude of the MODIS-LST product in detecting small agriculture areas; moreover, the surrounding targets exerts heavy influence on the central pixel by contaminating it, even more than in optical products (Deng & Wu, 2013), it is a property of the heat which is always changing towards the equilibrium. In short, sudden transitions between adjacent targets are unlikely to occur in thermal products.

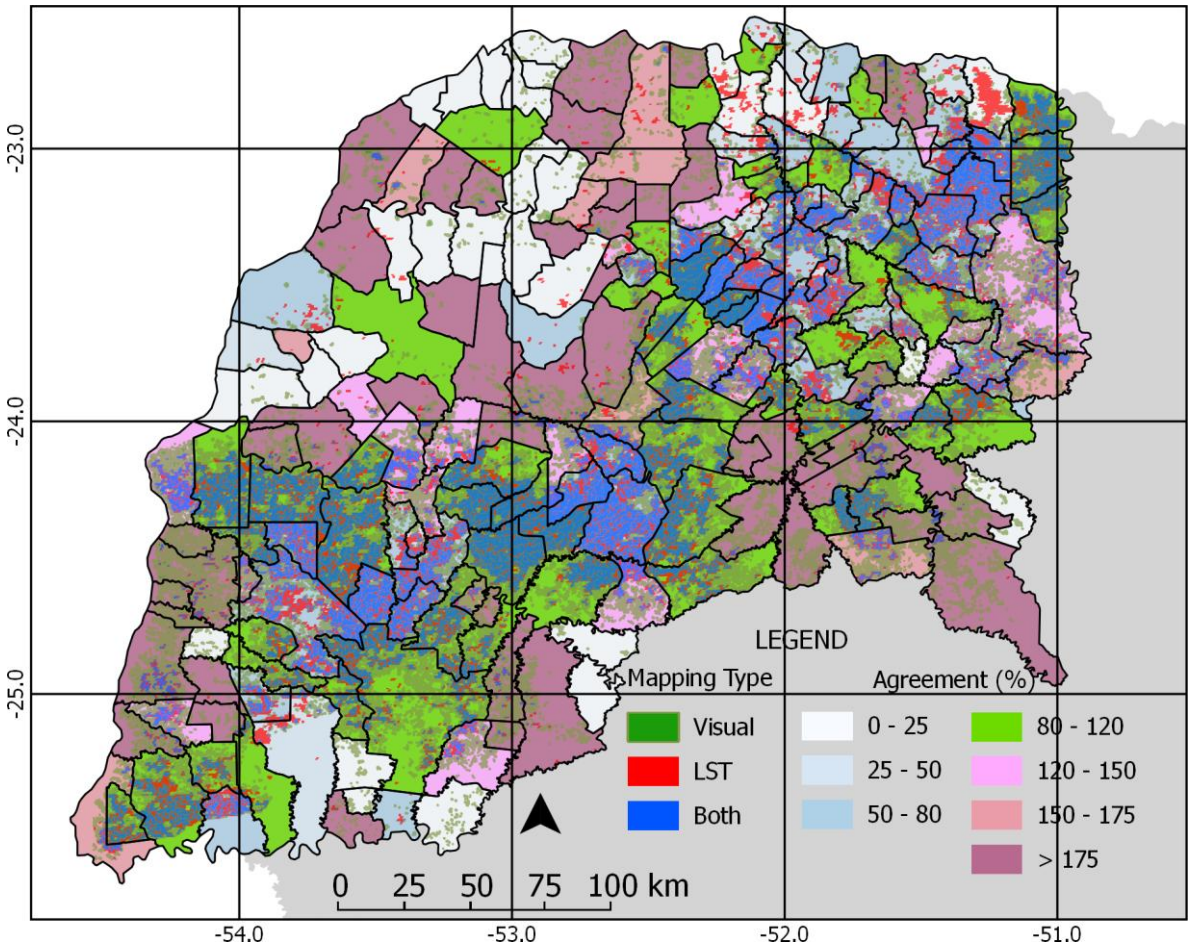

Figure 3- Agreement percentage between GESER/ESALQ-USP and the LST derived maps. The map also shows the annual agriculture areas detected visually, by LST method and by both.

We assessed the spatial agreement between methods by municipality. In order to avoid uncertainty related to area calculation, all layers were reprojected into Albers Equal Area Conic with standard parameters for Brazil as established by the Brazilian Institute of Geography and Statistics (IBGE). For the sake of brevity, the data were aggregated into microregions as shown in the Table 3.

From the Table 3 analysis, it is clear that the microregions whose texture soil is medium (Paranavaí, Umuarama, Cianorte and Ivaiporã) presented lower agreement between maps. This is due to the low annual agriculture acreage, so, simple commission or omission errors

lead to low agreement. Regions where there is abundance of annual agriculture occurrence (Floraí, Maringá, Porecatú and Apucarana) yielded better results. From the Figure 3 and Table 3 coupled analysis, we can conclude that the LST derived method performance is highly dependent on the adjacency of the crop areas. In short, the more aggregated the areas, the less susceptible to contamination, the more efficient is the LST derived method.

Table 3 – Spatial agreement between GESER and LST by microregion.

Microregion	None	GESER	LST	Both	GESER	LST
	hectares				%	%
Foz do Iguaçu	363872	48252	61336	62826	56.6	50.6
Cascavel	578268	95176	73382	105304	52.5	58.9
Toledo	359825	140844	137312	237384	62.8	63.4
Ivaiporã	459081	78586	31551	46159	37.0	59.4
Faxinal	145397	30282	23480	27403	47.5	53.9
Londrina	152361	46744	56014	90499	65.9	61.8
Apucarana	124736	22412	39811	40589	64.4	50.5
Maringá	62749	10197	41834	42598	80.7	50.5
Floraí	14386	7030	28679	79871	91.9	73.6
Porecatú	101977	16777	55768	62560	78.9	52.9
Astorga	358610	37523	64632	50323	57.3	43.8
Campo Mourão	326306	100416	96343	184051	64.7	65.6
Goioerê	209136	53210	56753	167508	75.9	74.7
Cianorte	350429	26728	15336	14972	35.9	49.4
Umuarama	922753	45814	24541	29874	39.5	54.9
Paranavaí	944538	38202	27685	5273	12.1	16.0

Note: The table represents the spatial agreement between classes in a dual way, as considering one source or the other as basis. *GESER(%)* represents the agreement between maps using *GESER* as basis and so on. *Both = GESER + LST*; *GESER(%) = Both / GESER*; *LST(%) = Both / LST*.

4. Conclusions

We proposed a method for mapping annual agriculture using only time-series analysis of MODIS-LST data. Further, to yield a representative image we relied on the calculation of the time-series variance which is effective in representing the time-series unsteadiness. This thermal approach were not yet in depth explored, thus, the present work brings new

findings about temperature and vegetation relationships over time. The proposed method does not proves itself on being more efficient on mapping agriculture than traditional VIs methods, however, on achieving good results, it proves that the thermal data can effectively translate biophysical attributes of vegetation using a different physical basis. The analysis showed that Forests has lower seasonal temperature variation than annual agriculture, pasture and sugarcane stay in the middle of this variance scale. So, for future works, Forests can be used as a proxy for assessing the climate variation over an area since it shows lower variance than the other targets, this helps to dissociate the thermal variability into climatic and phenological components.

The analysis let us conclude that the difference between daytime and nighttime temperatures is more suitable than daytime solely on dissociating land cover classes. Moreover, MODIS-Aqua data were more responsive to intra-daily temperature variation than MODIS-Terra due to the time of satellites passage over the area. Day temperature is usually higher at 13:30 than 10:30 due to the accumulated irradiance, for that reason Aqua showed better results.

As main drawback, the method performance is strongly influenced by neighbor contamination on a central pixel, so, the boundaries between classes are not so clear when compared to optical remote sensing. This is due to the low spatial resolution of the sensor and the fact that heat is physically always flowing towards equilibrium.

Indeed, despite the shortcomings, the proposed method uses non-traditional datasets for mapping achieving good results depending on the target. Moreover, this approach can be combined to the more traditional yielding better results and furthering the biophysical relations between vegetation and the electromagnetic spectrum.

References

Centro de Estudos Avançados em Economia Aplicada (CEPEA). (2014). PIB do Agronegócio Brasileiro.

Deng, C., & Wu, C. (2013). Examining the impacts of urban biophysical compositions on surface urban heat island: A spectral unmixing and thermal mixing approach. *Remote Sensing of Environment*, *131*, 262–274.

Ezzine, H., Bouziane, A., & Ouazar, D. (2014). Seasonal comparisons of meteorological and agricultural drought indices in Morocco using open short time-series data. *International Journal of Applied Earth Observation and Geoinformation*, *26*, 36–48.

Huete, A., Didan, K., Miura, T., Rodriguez, E. ., Gao, X., & Ferreira, L. . (2002). Overview of the radiometric and biophysical performance of the MODIS vegetation indices. *Remote Sensing of Environment*, *83*(1-2), 195–213.

Kogan, F. (1995). Droughts of the late 1980s in the United State as derived from NOAA data. *Bulletin of the American Meteorological Society*.

Kuenzer, C., & Dech, S. (Eds.). (2013). *Thermal Infrared Remote Sensing* (Vol. 17, p. 537). Dordrecht: Springer Netherlands.

Lambin, E. F., & Ehrlich, D. (1996). The surface temperature-vegetation index space for land cover and land-cover change analysis. *International Journal of Remote Sensing*, *17*(3), 463–487.

Murray, T., & Verhoef, A. (2007). Moving towards a more mechanistic approach in the determination of soil heat flux from remote measurements. *Agricultural and Forest Meteorology*, *147*(1-2), 80–87.

Nemani, R., & Running, S. (1997). Land cover characterization using multitemporal red, near-IR, and thermal-IR data from NOAA/AVHRR. *Landscape Parametrization*, *7*(February), 79–90.

Rhee, J., Im, J., & Carbone, G. J. (2010). Monitoring agricultural drought for arid and humid regions using multi-sensor remote sensing data. *Remote Sensing of Environment*, *114*(12), 2875–2887.

Rouse, J. W., Haas, R. H., & Schell, J. A. (1974). *Monitoring the vernal advancement and retrogradation (greenwave effect) of natural vegetation*. Texas A & M University.

Rudorff, B. F. T., Adami, M., Aguiar, D. A., Moreira, M. A., Mello, M. P., Fabiani, L., … Pires, B. M. (2011). The Soy Moratorium in the Amazon Biome Monitored by Remote Sensing Images. *Remote Sensing*, *3*(12), 185–202.

Sandholt, I., Rasmussen, K., & Andersen, J. (2002). A simple interpretation of the surface temperature/vegetation index space for assessment of surface moisture status. *Remote Sensing of Environment*, *79*(2-3), 213–224.

Tang, H., & Li, Z.-L. (2014). *Quantitative Remote Sensing in Thermal Infrared* (p. 281).

Berlin, Heidelberg: Springer Berlin Heidelberg.

Tucker, C. J. (1979). Red and photographic infrared linear combinations for monitoring vegetation. *Remote Sensing of Environment*, *8*(2), 127–150.

Wan, Z. (2008). New refinements and validation of the MODIS Land-Surface Temperature/Emissivity products. *Remote Sensing of Environment*, *112*(1), 59–74.

Wan, Z., & Li, Z. (1997). A physics-based algorithm for retrieving land-surface emissivity and temperature from EOS/MODIS data. *IEEE Transactions on Geoscience and Remote Sensing*, *35*(4), 980–996.

Wan, Z., Wang, P., & Li, X. (2004). Using MODIS Land Surface Temperature and Normalized Difference Vegetation Index products for monitoring drought in the southern Great Plains, USA. *International Journal of Remote Sensing*, *25*(1), 61–72.

Wang, K., Li, Z., & Cribb, M. (2006). Estimation of evaporative fraction from a combination of day and night land surface temperatures and NDVI: A new method to determine the Priestley–Taylor parameter. *Remote Sensing of Environment*, *102*(3-4), 293–305.

Wardlow, B. D., & Egbert, S. L. (2008). Large-area crop mapping using time-series MODIS 250 m NDVI data: An assessment for the U.S. Central Great Plains. *Remote Sensing of Environment*, *112*(3), 1096–1116.

Xiao, X., Boles, S., Liu, J., Zhuang, D., Frolking, S., Li, C., … Moore, B. (2005). Mapping paddy rice agriculture in southern China using multi-temporal MODIS images. *Remote Sensing of Environment*, *95*(4), 480–492.